# Anisotropy of Frictional Forces in Muscovite Mica

Motohisa Hirano[(a)]
*Interdisciplinary Research Laboratories, Nippon Telegraph and Telephone Corporation, Musashino, Tokyo 180, Japan*

Kazumasa Shinjo[(b)]
*ATR Optical Radio Communications Research Laboratories, Seika-cho, Soraku-gun, Kyoto 619-02, Japan*

Reizo Kaneko
*Interdisciplinary Research Laboratories, Nippon Telegraph and Telephone Corporation, Musashino, Tokyo 180, Japan*

Yoshitada Murata
*Institute for Solid State Physics, University of Tokyo, 7-22-1, Roppongi, Minato, Tokyo 106, Japan*
(Received 6 February 1991; revised manuscript received 27 June 1991)

The static and dynamic frictional forces of single-crystal muscovite mica are measured as a function of the lattice misfit angle between the two contacting cleavage lattices at a very light load under both dry and ambient atmospheres. The frictional forces are anisotropic with respect to the lattice misfit angle, i.e., they increase (decrease) when the contacting surfaces approach being commensurate (incommensurate). The underlying mechanisms of the anisotropy are discussed in terms of the commensurability between the contacting lattices.

PACS numbers: 46.30.Pa

The frictional properties of various single crystals have been measured, and it has been shown that the frictional forces of some crystals are anisotropic with respect to the crystallographic direction of sliding [1-4]. For example, when sliding the {001} planes of a single-crystal diamond against another in air, the frictional force is smaller for sliding in the ⟨110⟩ direction than in the ⟨100⟩ direction by a factor of $\frac{2}{3}$ [1]. The clean surfaces of some hexagonal metals showed the anisotropy, in which the frictional force of the {0001} planes in the ⟨11$\bar{2}$0⟩ direction was smaller than that of the {10$\bar{1}$0} planes in the ⟨11$\bar{2}$0⟩ direction by a factor of $\frac{1}{2}$, when sliding single-crystal cobalt against polycrystalline cobalt [2]. Some other materials such as copper [3] and ceramics [4] have also shown frictional anisotropy, depending on the crystallographic direction of sliding.

Plastic deformations and fractures were observed at the rubbed surfaces when the anisotropy appeared in the above systems, and the mechanisms of the observed anisotropy were analyzed by examining the preferred slip system in single crystals. The anisotropy of diamond was interpreted by the preferred slip system in which ⟨110⟩ sliding is more likely than ⟨100⟩ sliding to yield the critical resolved shear stress that activates the lattice slip and the subsequent crack formation on the primary slip plane, which was assumed to be {111} [1]. The anisotropy disappeared at very small loads, i.e., when the contact condition approached being elastic below the determined critical mean contact pressure [1].

This Letter reports the first observation of frictional anisotropy in muscovite mica by measuring the frictional forces at very small load as a function of the lattice misfit angle between the two contacting lattices. The underlying mechanisms of the observed frictional anisotropy are examined in connection with our theoretical conclusion on the effects of the commensurability between contacting lattices [5]. It is shown that the frictional forces are anisotropic with respect to the lattice misfit angle, i.e., they increase (decrease) when the contacting surfaces approach being commensurate (incommensurate). From studying how introducing dirtiness into the contacting surfaces affects the frictional forces and from measuring the highly resolved surface roughness of the mica cleavage surfaces, it is concluded that the observed anisotropy stems from the change in commensurability of contacting lattices.

Muscovite mica is suitable for our purpose since it is a relatively large single crystal and its cleavage surface has few steps, being atomically flat. Mica surfaces have been successfully used for measuring frictional forces [6] and adhesive forces [7]. The lattice orientations were determined by x-ray diffraction prior to friction testing. X-ray diffractometer experiments confirmed that mica has a monoclinic structure, whose space group is $C_{2h}^6$ [8]. Figure 1(a) shows the back-reflection Laue pattern of the mica in approximately the [001] direction. Figure 1(b) shows the corresponding map representing lines made by a set of reciprocal-lattice points of zone planes, denoted ($hkl$), belonging to the zone axes, denoted [$hkl$]. Several of these patterns were examined at different points over a 1-cm$^2$ area on the sample. The Laue patterns were nearly invariant at the different points, implying that the mica used is a relatively large single crystal over the 1-cm$^2$ area. The lattice orientation of the cleavage surface was determined by specifying the primitive vector **b** perpendicular to the line made by a set of reciprocal points of zone planes belonging to the zone axis denoted [010] in the map shown in Fig. 1(b).

 

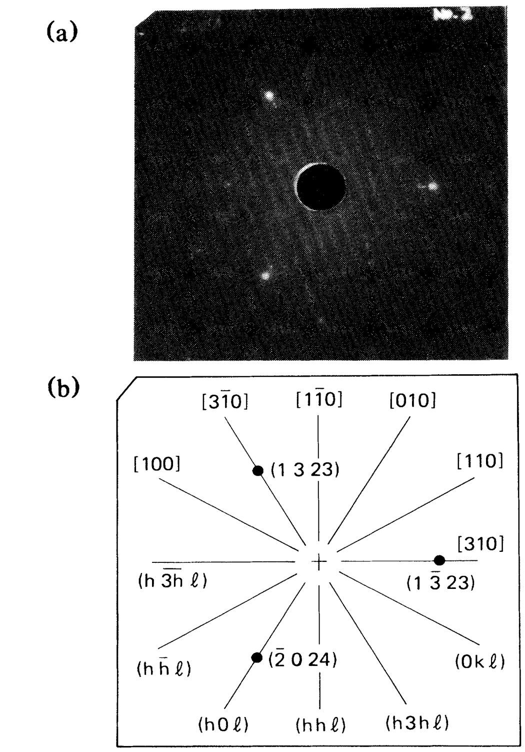


FIG. 1. (a) Back-reflection Laue pattern of muscovite mica. (b) Map showing lines made by a set of reciprocal points of zone planes. The angles between zone axes [010] and [110], and between [010] and [310], are, respectively, 29.89° and 59.89°. The representative diffraction spots are identified as (1323), (1$\bar{3}$23), and ($\bar{2}$024). The high intensities are due to satisfying the first-order diffraction condition.

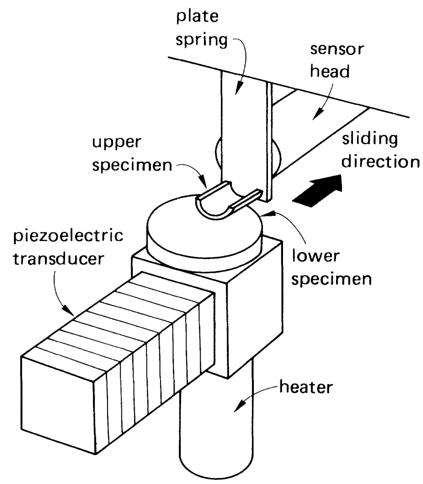


FIG. 2. Schematic illustration of friction-measuring apparatus. The sliding direction is shown by the arrow corresponding to the direction of extension of the piezoelectric transducer. Movement per unit voltage of the peizoelectric transducer is 0.18 $\mu$m/V. The resolution of the measured frictional force is estimated to be $1\times10^{-6}$ N according to the 0.1-$\mu$m spatial resolution of the capacitance displacement meter.

Figure 2 shows the schematic setup for the measurement. Two mica sheets were cut from a larger sheet as carefully as possible to make the edges of the mica sheets smooth. One sheet was attached to a cylindrically curved substrate with an 8-mm radius and 5-mm length (upper specimen), and the other, to a disk substrate with a 10-mm diameter (lower specimen). Friction was measured under an argon-purged dry atmosphere with controlled water vapor pressure and at a raised surface temperature [9] (over 100 °C) to reduce the thickness of contaminants such as water and organic compounds on the cleavage surfaces. The mica sheets were cleaved again after finally attaining the lowest water vapor pressure in the chamber. The upper specimen was then placed on the lower specimen at a load corresponding to its own weight ($1.2\times10^{-3}$ N); this gave an elastic contact zone of 0.25 $\mu$m by 5 mm and a mean contact pressure of 0.9 MPa according to the measured elastic constants [10].

Static and dynamic frictional forces were measured between the two contacting specimens during one traverse of a few $\mu$m. First, both the upper and lower specimens were moved by extending the piezoelectric transducer at a speed of 2.7 $\mu$m/s toward the thin plate spring (5 $\times15\times0.1$ mm$^3$), whose spring constant is 30.6 N/m. As the two specimens approached the plate spring, only the upper specimen touched the spring. The deflection of the spring was monitored using a displacement meter to detect the change in capacitance between the plate spring and the displacement meter sensor head. When the spring force overcame the frictional force, sliding occurred. The spring force during sliding determined the static and dynamic frictional forces. A detailed description of the setup will be published elsewhere.

The change in the measured static and dynamic frictional forces with the lattice misfit angle $\theta$, the angle between the two contacting mica lattices, is shown in Fig. 3. The two specimens were brought into contact such that each primitive vector **a** corresponded to the sliding direction shown in Fig. 3. In a dry atmosphere with a relative water vapor pressure $p/p_0\sim9\times10^{-5}$ and at a surface temperature of 130 °C, the static and dynamic frictional forces show the anisotropy in which the frictional forces increase as the misfit angle approaches $\theta=0°$ or 60°, and decrease as it approaches $\theta=30°$. Alternatively, they increase (decrease) when the contacting surfaces approach being commensurate (incommensurate). The static frictional force ranges from 2.2 to $7.6\times10^{-4}$ N. The changes in the frictional forces seem to have sixfold symmetry, reflecting the pseudohexagonal symmetry of the cleavage surfaces, which are defined as the potassium layer sandwiched between the two hexagonal sheets of silicate tetrahedra. The measured atomic parameters showed the mica structure to be slightly distorted from the ideal structure by a departure from hexagonal symmetry on the surface of the silicate sheets [11]. However,

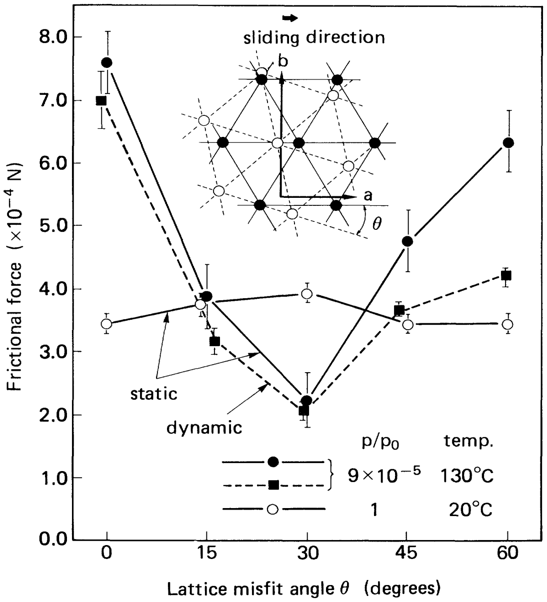


FIG. 3. The change in the measured static and dynamic frictional forces as a function of the lattice misfit angle $\theta$ between two contacting mica lattices. The misfit angle is approximately 0° when the two specimens are brought into commensurate contact without rotation of the lower specimen.

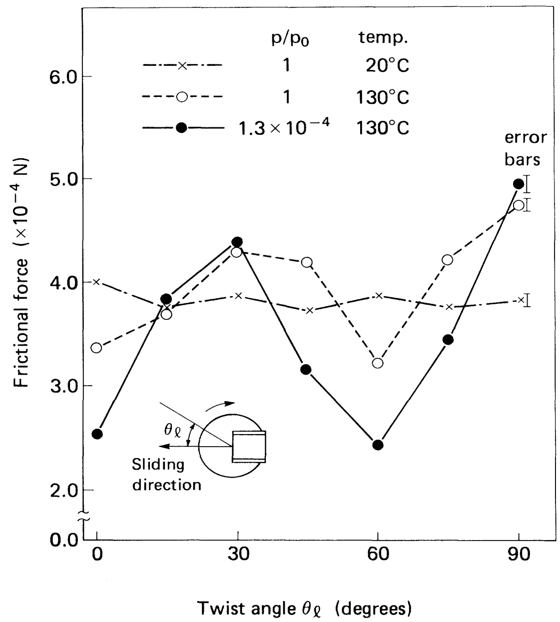


FIG. 4. The change in the measured static frictional force as a function of twist angle $\theta_l$ between the two contacting specimens.

no frictional anisotropy can be seen in the ambient atmosphere in Fig. 3. This can be due to the introduction of dirtiness (water) to the contacting surfaces. McGuiggan and Israelachvili [7] observed the anisotropy of the adhesion energy between two contacting mica cleavage surfaces in distilled water and in aqueous KCl. The results showed the adhesion peaks at specific angles corresponding to crystallographic atomic alignment ($\theta = 0°$, 60°, 120°, and 180°). However, their observation cannot be directly related to our observed anisotropy because of the different atmosphere where the measurements were done. Their results were explained by the excess surface energy of a low-angle grain boundary. On the other hand, they observed no anisotropy of adhesion energy in an $N_2$ environment at a relative humidity of 33%, corresponding to our results showing no frictional anisotropy in ambient air.

The static frictional forces are shown in Fig. 4 as a function of the twist angle between the two contacting specimens with different relative water vapor pressures and at different surface temperatures. Here, the lattice orientations of the upper and lower specimens were measured, but not specified with respect to the sliding direction, i.e., each primitive vector **a** does not necessarily correspond to the sliding direction, while the lattice orientation of both surfaces were initially matched at the twist angle $\theta_l = 0°$. Figure 4 shows the anisotropy of the static frictional force, which ranges from 2.5 to $5.0 \times 10^{-4}$ N over $\theta_l = 0°$ to 90° under a dry atmosphere and at a high surface temperature. The average thickness of the water layer adsorbed on the mica cleavage surfaces can be less than a few Å, i.e., the cleavage surfaces are clean, under an extremely low relative water vapor pressure $p/p_0$ of $9 \times 10^{-5}$, according to the measurement made on a cleavage surface of lithium fluoride using ellipsometry, in which the average water layer thickness was negligibly small below $p/p_0 \sim 0.3$ [12]. By increasing the relative water vapor pressure and subsequently decreasing the surface temperature, it is seen in Fig. 4 that the anisotropy gradually weakens, and then disappears under an ambient atmosphere.

The mean contact pressure of 0.9 MPa at the mica contacting surfaces is 3 orders smaller than the values of 0.4 GPa at cobalt surfaces [2] and 0.3 GPa at copper surfaces [3]. This suggests that the contact condition of the mica might be elastic if one takes into consideration that the elastic constant $c_{44}$ of 12 GPa [10] for mica is comparable in magnitude to that of 75 GPa [10] for cobalt and copper. The topographies of the contacting surfaces were measured before and after sliding by both an atomic force microscope (AFM) [13] over a 5-nm by 5-nm scan and by a point contact microscope (PCM) [14] over a 2000-nm by 2000-nm scan. The as-cleaved mica surfaces were flat on an atomic scale, within 0.2-nm resolution, according to the AFM measurements in repulsive mode. The atomically resolved periodic variation in the surface force was obtained by scanning a sharp silicon nitride tip [15]. The PCM images showed no topographical changes, within a 2-nm resolution, between before and after sliding. Thus appreciable plastic deformations and fractures were unlikely to occur at the sliding mica surfaces. This implies that the contact condition of mica is elastic, which is different from the plastic contact in the previously observed frictional anisotropy [1–4].

It was shown that the static and dynamic frictional forces between contacting mica cleavage surfaces increase when the surfaces approach being commensurate, and decrease when incommensurate. In a previous paper [5], we proposed new mechanisms for the atomistic origin of static and dynamic frictional forces by theoretically studying a three-dimensional many-particle system, in which clean and flat surfaces contact elastically. Our picture explained how the static frictional force appears in terms of interatomic potentials and atomic configurations of surfaces, and how the given translational energy of a sliding body is dissipated in dynamic friction. It was concluded that the frictional force appears when contacting surfaces are commensurate, and that they vanish when those are incommensurate. Therefore, the observed frictional anisotropy in mica is consistent with our theoretical conclusion [5]. Erlandsson *et al.* [6] observed the atomic-scale periodic change in the frictional forces of mica by scanning a polycrystalline tungsten sharp tip on a mica cleavage surface. They also remarked on the potential importance of the commensurability of contacting surfaces as a cause of their observed periodic change.

The frictionless state has been discussed for the case of weak interfacial interactions such as van der Waals interaction [16,17]. We derived the criterion for the occurrence of the frictionless state in a three-dimensional many-particle system [5]. The threshold of interfacial interaction strength for which frictional forces vanish was determined for cubic metals [5]. Consequently, we have concluded that a frictionless state appears for a wider class of interfacial potentials including strong interactions such as metallic bonding, i.e., the state of *superlubricity* exists in realistic systems [5].

It is clear from Fig. 4 that the frictional forces become small as surfaces are cleaned when contacting incommensurately. We then expect to observe much smaller frictional forces by preparing more well-defined surfaces. However, our observed lowest frictional force at $\theta = 30°$ (when incommensurate) shown in Fig. 3 is not so small. This might be due to some deviation from perfect cleanliness and perfect periodicity over the contacting area. Experiments using the well-defined surfaces under a high vacuum of $10^{-11}$ Torr will be reported in the future.

In conclusion, the frictional forces of muscovite mica were measured as a function of the lattice misfit angle between the two contacting cleavage lattices, and it was found that the frictional forces are anisotropic with respect to the lattice misfit angle, i.e., they increase (decrease) when the surfaces approach being commensurate (incommensurate). The observed frictional anisotropy stems from the change in the commensurability between contacting lattices, implying the existence of the state of *superlubricity* [5].

We wish to thank Professor K. Suzuki, Professor H. Kamiya, and Professor N. Sasada for their technical advice.

[a]Electronic address: hirano%aela.ntt.jp@relay.cs.net.
[b]Electronic address: shinjo%atr-rd.atr.co.jp.

[1] Y. Enomoto and D. Tabor, Proc. R. Soc. London A **373**, 405 (1981).
[2] D. H. Buckley, ASLE Trans. **11**, 89 (1968).
[3] R. Takagi and Y. Tsuya, Wear **4**, 216 (1961); Y. Tsuya, Wear **14**, 309 (1969).
[4] D. H. Buckley and K. Miyoshi, in *Structural Ceramics,* edited by J. B. Watchman, Jr. (Academic, San Diego, CA, 1989), Vol. 29, p. 300.
[5] M. Hirano and K. Shinjo, Phys. Rev. B **41**, 11 837 (1990); K. Shinjo and M. Hirano (to be published).
[6] R. Erlandsson, G. Hadziioannou, C. M. Mate, G. M. McClelland, and S. Chiang, J. Chem. Phys. **89**, 5190 (1988).
[7] P. M. McGuiggan and J. N. Israelachvili, Chem. Phys. Lett. **149**, 469 (1988); J. Mater. Res. **5**, 2232 (1990).
[8] W. L. Bragg, *Atomic Structure of Minerals* (Cornell Univ. Press, Ithaca, 1937), p. 205.
[9] The surface temperature was determined using a radiation thermometer to measure the temperature of a black tape, whose emissivity is approximately 1.0, stuck onto the mica cleavage surface.
[10] G. Simmons and H. Wang, *Single Crystal Elastic Constants and Calculated Aggregate Properties* (MIT, Cambridge, MA, 1971).
[11] E. W. Radoslovich, Acta Cryst. **13**, 919 (1960).
[12] K. Kinoshita, H. Kojima, and H. Yokota, Jpn. J. Appl. Phys. **1**, 234 (1962).
[13] G. Binnig, C. F. Quate, and Ch. Gerber, Phys. Rev. Lett. **56**, 930 (1986).
[14] R. Kaneko, S. Oguchi, T. Miyamoto, Y. Andho, and S. Miyake, Soc. Tribol. Lubr. Eng., Special Publication SP-29.
[15] B. Drake *et al.*, Science **243**, 1586 (1989).
[16] J. B. Sokoloff, Surf. Sci. **144**, 267 (1984); Phys. Rev. B **31**, 2270 (1985).
[17] G. M. McClelland, in *Adhesion and Friction,* edited by M. Grunze and H. J. Kreuzer, Springer Series in Surface Science Vol. 17 (Springer-Verlag, Berlin, 1990), p. 1.

(a)

(b)

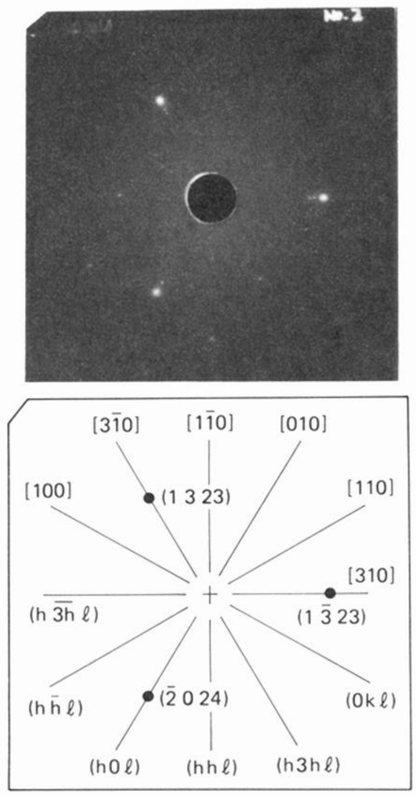


FIG. 1. (a) Back-reflection Laue pattern of muscovite mica. (b) Map showing lines made by a set of reciprocal points of zone planes. The angles between zone axes [010] and [110], and between [010] and [310], are, respectively, 29.89° and 59.89°. The representative diffraction spots are identified as (1 3 23), (1 $\bar{3}$ 23), and ($\bar{2}$ 0 24). The high intensities are due to satisfying the first-order diffraction condition.